Title

Activation of Parathyroid Hormone 2 Receptor Induces Decorin Expression and Promotes Wound Repair

Journal

Journal of Investigative Dermatology, 137(8)

ISSN

0022-202X

Authors

Sato, Emi

Zhang, Ling-juan

Dorschner, Robert A

et al.

Publication Date

2017-08-01

DOI

10.1016/j.jid.2017.03.034

Peer reviewed

Accepted Manuscript

Activation of parathyroid hormone 2 receptor induces decorin expression and promotes wound repair

Emi Sato, Ling-juan Zhang, Robert A. Dorschner, Christopher A. Adase, Biswa P. Choudhury, Richard L. Gallo

PII: S0022-202X(17)31424-0

DOI: 10.1016/j.jid.2017.03.034

Reference: JID 835

To appear in: *The Journal of Investigative Dermatology*

Received Date: 5 December 2016

Revised Date: 25 March 2017

Accepted Date: 27 March 2017

Please cite this article as: Sato E, Zhang L-j, Dorschner RA, Adase CA, Choudhury BP, Gallo RL, Activation of parathyroid hormone 2 receptor induces decorin expression and promotes wound repair, *The Journal of Investigative Dermatology* (2017), doi: 10.1016/j.jid.2017.03.034.

Activation of parathyroid hormone 2 receptor induces decorin expression and promotes wound repair

Emi Sato[1], Ling-juan Zhang[1], Robert A Dorschner[1], Christopher A Adase[1], Biswa P Choudhury[2], Richard L Gallo[1].

[1]Department of Dermatology, University of California San Diego, La Jolla, CA, 92093
[2]Glycotechnology Core Resource, University of California San Diego, La Jolla, CA, 92093

Short title: Pth2r signaling induces decorin expression

Abbreviations: cAMP response element-binding protein (CREB); cyclic AMP (cAMP); decorin; extracellular matrix (ECM); G protein-coupled receptor (GPCR); parathyroid hormone (PTH); PTH second Receptor (PTH2R); tuberoinfundibular peptide of 39 residues (TIP39); glycosaminoglycans (GAG); proteoglycans (PG); chondroitin sulfate (CS); dermatan sulfate (DS); heparan sulfate (HS); extracellular matrix (ECM);matrix metalloproteases (MMPs); three-dimensional (3D)

Corresponding author:
Richard L Gallo,
Department of Dermatology
University of California San Diego
9500 Gillman Dr.,#0869,
La Jolla, California, 92093
USA.
Email: rgallo@ucsd.edu

ABSTRACT

In this study, we report that tuberoinfundibular peptide of 39 residues (TIP39), a parathyroid hormone ligand family member that was recently identified to be expressed in the skin, can induce decorin expression and enhance wound repair. Topical treatment of mice with TIP39 accelerated wound repair while TIP39-deficient mice had delayed repair that was associated with formation of abnormal collagen bundles. To study the potential mechanism responsible for the action of TIP39 in the dermis, fibroblasts were cultured in three-dimensional (3D) collagen gels, a process that results in enhanced decorin expression unless activated to differentiate to adipocytes, whereupon these cells reduce expression of several proteoglycans, including decorin. siRNA-mediated silencing of parathyroid hormone 2 receptor (PTH2R), the receptor for TIP39, suppressed the expression of ECM-related genes, including decorin, collagens, fibronectin and matrix metalloproteases. Skin wounds in TIP39-/- mice had decreased decorin expression while addition of TIP39 to cultured fibroblasts induced decorin and increased phosphorylation and nuclear translocation of CREB. Fibroblasts differentiated to adipocytes and treated with TIP39 also showed increased decorin and production of chondroitin sulfate. Furthermore, the skin of PTH2R-/- mice showed abnormal ECM structure, decreased decorin expression and skin hardness. Thus, the TIP39-PTH2R system appears to be a previously unrecognized mechanism for regulation of ECM formation and wound repair.

INTRODUCTION

The extracellular matrix (ECM) contains fibrillar collagens, glycosaminoglycans (GAGs) and proteoglycans (PGs), and provides support and anchorage for cells. It regulates cell polarity, differentiation and adhesion, protects against infection and ultraviolet light damage, and supports wound healing (Gallo et al., 1994; Naylor et al., 2011; Rostand and Esko, 1997; Trowbridge and Gallo, 2002). In the skin, the main source of ECM is thought to be dermal fibroblasts, but a recent study suggests that adipocytes also regulate ECM and may influence wound healing (Schmidt and Horsley, 2013). Decorin is a major ECM macromolecule and a member of the widely distributed small leucine-rich proteoglycans family. It is thought to have important functions in tissue assembly (Danielson et al., 1997). The common features of this family are core proteins containing two cysteine clusters flanking a leucine-rich repeat domain and the presence of an ear-repeat C-terminal motif (Schaefer and Schaefer, 2010). Decorin bears one dermatan sulfate or chondroitin sulfate (CS) side chain in the N-terminal region.

Decorin is notable as a regulator of collagen fibrillogenesis through its interaction with collagen triple helices to regulate their spacing within a fibril (Edwards, 2012; Weber et al., 1996). We previously reported that switching fibroblasts from growth on type I collagen in a monolayer to a three-dimensional (3D) collagen gel induced decorin expression (Lee et

al., 2004). Mice harboring a targeted disruption of the decorin gene are viable but have fragile skin with markedly reduced tensile strength (Danielson et al., 1997). These phenomena suggest that decorin may have important roles in the proliferative and remodeling phases of wound healing, because new collagen fibrils are secreted from fibroblasts to make a strong scar during these phases (Brett, 2008). Supporting this conclusion, decorin deficient mice have been shown to have abnormal wound repair (Jarvelainen et al., 2006).

Tuberoinfundibular peptide of 39 residues (TIP39) is a member of the parathyroid hormone (PTH) ligand family, and an agonist of the PTH 2 receptor (PTH2R). PTH2R is a class B G protein-coupled receptor (Usdin et al., 1999), which can stimulate both the $G\alpha_s$–adenylyl cyclase and $G\alpha_q$–phospholipase C pathways (Ritter and Hall, 2009). PTH, another PTH2R agonist, phosphorylates cAMP response element-binding protein (CREB) (Atfi and Baron, 2010; Qiu et al., 2010), and phosphorylation of CREB induces decorin transcription (Akhurst, 2006; Wahab et al., 2000). Previously, we reported that TIP39 is expressed in both the epidermis and differentiated subcutaneous adipocytes, and that it regulates intracellular calcium and affects keratinocyte differentiation (Sato et al., 2016). Furthermore, TIP39 upregulates expression of the fibronectin 1 (*FN1*), matrix metalloprotease 13 (*MMP13*) and collagen type I alpha 2 (*COL1A2*) genes in PTH2R-overexpressing chondrocytes (Panda et al., 2009). Collagen and matrix metalloproteases (MMPs) also act in the inflammatory and

remodeling phases of wound healing (Brett, 2008). Based on these results, we predicted that TIP39–PTH2R signaling may affect dermal ECM and keratinocyte migration, and thereby enhance wound repair. In this study, we hypothesized that in addition to the effects previously shown on keratinocytes, TIP39–PTH2R signaling may also influence wound repair through action on the production of decorin and other ECM components by fibroblasts and adipocytes in the dermis.

RESULTS

TIP39 enhances wound repair

To investigate the effects of TIP39 on mouse excisional wound repair we performed daily injections of 250 ng TIP39 in the skin of mice, and observed significantly enhanced closure on days 2 and 4 compared to vehicle injections (**Figure 1a and Figure S1a**). Similarly, TIP39 knockout mice ($Tip39^{-/-}$) showed a delayed rate of closure from day 2 to 8 (**Figure 1b and 1c**). Van Gieson staining of day 7 wound samples from TIP39-/- and littermate control heterozygous mice (TIP39+/-) showed that collagen fiber bundles in TIP39-/- wounds were thicker than in TIP39+/- wounds (Figure 1d and Supplemental Figure 1b). Furthermore, wound re-epithelialization as measured in a splinted-wound model also suggested that re-epithelialization of TIP39-/- wounds was delayed compared with their heterozygous controls (Figure 1e, 1f and Figure S1d).

PTH2 receptor signaling regulates the extracellular matrix

To understand how the presence of TIP39 or its receptor might influence wound repair, we next investigated the effects of PTH2R signaling in several cultured cell types, including keratinocytes, endothelial cells, fibroblasts and adipocytes. Both TIP39 and PTH2R expression were highest in adipocytes (**Figure 2a**). Transfection of a short interfering RNA

(siRNA) targeting PTH2R into human fibroblast-like adipocyte precursor cells and adipocytes was effective to suppress PTH2R gene expression by >90% for both cell types (**Figure 2b and Figure S1e**) and whole transcriptome analysis by RNA sequencing showed that PTH2R silencing significantly downregulated 46 genes in fibroblasts and 252 genes in differentiated adipocytes (**Figure 2c**). Gene ontology (GO) enrichment analysis showed that PTH2R silencing had strong effects on the regulation of ECM in fibroblasts (**Figure 2d**). **Figure 2e and 2f** illustrates significantly downregulated genes by gene ontogeny analysis (GO): 0030198 (ECM organization). We focused on decorin (*DCN*) and collagen type I alpha 1 (*COL1A1*) for the rest of this study because type I collagen is highly abundant in the skin and decorin is well known to modulate the regularity of collagen fibrils and is related to skin fragility (Birk and Silver, 1984; Danielson et al., 1997; Scott and Orford, 1981), and may therefore be relevant to the wound healing phenotype observed in Figure 1.

TIP39 enhances the production of decorin from fibroblasts in three-dimensional collagen gels

TIP39-/- mice showed less decorin and MMP13 mRNA expression compared with wounded skin from heterozygous littermates (**Figure 3a** and **Figure S1c**). Because fibroblasts produce more decorin when incubated in 3D type I collagen gels (Lee et al., 2004), we established a 3D collagen culture model in which the mouse fibroblast cell line, 3T3-L1, could be

differentiated into adipocytes (**Figure S2a**). Differentiation medium, which contains dexamethasone, insulin and isobutylmethylxanthine, was added to the 3D cultures from 2 days after gel formation. Differentiation was confirmed by upregulation of the adiponectin gene (*Adipoq*) (**Figure S2d**) and by perilipin expression (**Figure S2c**). TIP39 suppressed *Adipoq* expression from day 2 to 6, but had no effect on day 7 (**Figure S2e**). Interestingly, decorin expression was suppressed by adipocyte differentiation (**Figure S2f**), but TIP39 increased decorin production in both undifferentiated fibroblasts and adipocytes in 3D collagen gels (**Figure 3b and 3c**).

TIP39 phosphorylates CREB and induces decorin transcription

We next investigated whether TIP39 might affect decorin production via the phosphorylation of CREB in mouse fibroblasts. TIP39 (1.5 μM) increased phosphorylated CREB (pCREB) in the nuclear fraction within 15 min after stimulation (**Figure 4a and 4b**). Glyceraldehyde 3-phosphate dehydrogenase (GAPDH) was used as a housekeeping protein (loading control) for the cytoplasmic fraction, and Lamin B was used for the nuclear fraction. **Figure 4c** shows immunostaining of pCREB (green) and nuclei (blue) after stimulation with 1 μM TIP39. As in **Figure 4a**, TIP39 induced the translocation of pCREB into the nucleus 15 min after stimulation (**Figure 4d)**. TIP39 treatment also resulted in accumulation of Decorin in a perinuclear location within 4h after TIP39 addition (**Figure 4e**).

Effects of TIP39 on adipocyte glycosaminoglycans

As a PG, decorin typically contains CS GAG side chains in the form of dermatan sulfate (DS) linked to its N-terminal region, and also has three potential sites for N-glycosylation in its protein core (Edwards, 2012; Seo et al., 2005). Monosaccharide composition analysis of the supernatant from differentiated adipocytes grown as monolayers showed that they mainly secreted disaccharides consistent with CS/DS (**Figure 5a, b**). Comparison of GAG production by gel electrophoresis and selective enzymatic digestion techniques of pre-adipocyte fibroblasts and adipocytes revealed that 3D collagen gels containing undifferentiated fibroblasts produced yellow-stained material that was digested by heparinase, indicative of heparan sulfate (HS) (**Figure 5c**, lanes A and B). Production of these materials was clearly reduced in gels containing differentiated adipocytes, which instead mainly produced purple-stained materials that were digested by chondroitinase ABC (**Figure 5c,** lanes C and D). Thus, undifferentiated fibroblasts mainly produced HS and differentiated adipocytes mainly produced CS. These changes in GAG composition suggest that GAGs may have an important role in adipocyte differentiation.

We next investigated the expression of various genes encoding HS or CS core proteins (Sarrazin et al., 2011) by quantitative polymerase chain reaction (qPCR) assays (**Figure 5d**). Adipocyte differentiation downregulated the expression of agrin (*Agrn*),

glypican1 (*Gpc1*) and glypican2 (*Gpc2*), known core proteins of HS. TIP39 significantly increased the expression of decorin (*Dcn*) in fibroblast and betaglycan (*Tgfbr3*) in adipocyte, both are known to contain CS (**Figure 5d**).

The lack of PTH2R signaling suppresses decorin expression in the mouse dermis

Finally, we investigated the expression of decorin in PTH2R-deficient murine skin. *Pth2r*-/- dermis expressed lower levels of decorin, as determined by immunofluorescence staining (**Figure 6a**). To quantify decorin expression in the mouse dermis and subcutaneous tissue, we separated epidermis by 0.5 M ammonium thiocyanate treatment. Decorin gene expression was suppressed in *Pth2r*-/- dermis and subcutaneous tissue (**Figure 6b**). Western blotting data showed that decorin protein expression was also suppressed (**Figure 6c**). Chondroitinase ABC digestion reduced the size of decorin from approximately 65 kDa to 50 kDa (**Figure 6c**, right lane). Transmission electron microscopy of collagen fibrils in the *Pth2r*-/- reticular dermis identified irregular collagen fibrils in these mice (**Figure 6d**) that are similar to those previously seen in decorin deficient mouse skin (Danielson et al., 1997). Furthermore, skin hardness measurements of *Pth2r*-/- mice showed that the overall compressibility of the skin from mice lacking the TIP39 receptor is softer than wild type mice (**Figure 6e**).

DISCUSSION

The study of GAGs and PGs has improved our understanding of cellular proliferation, differentiation, migration and wound healing (Trowbridge and Gallo, 2002). We showed in this study that TIP39 and PTH2R induced decorin expression in the dermis and appears to influence the structural organization of the ECM. These effects were associated with improved wound repair upon addition of TIP39, and deficient wound repair in the absence of either TIP39 or PTH2R. Since decorin regulates collagen fibrillogenesis by interacting with collagen triple helices to regulate spacing within fibrils (Edwards, 2012; Weber et al., 1996), and a lack of decorin results in increased skin fragility and deficient wound repair due to these abnormal collagen fibrils (Danielson et al., 1997), the phenotypes observed by altering the TIP39 signaling pathway are consistent with an important role for TIP39 in regulation of decorin. To our knowledge this is the first observation that a member of the PTH family has a direct influence on ECM production in the dermis.

Analysis of the transcriptional response of fibroblasts and adipocytes after the silencing of *PTH2R*, after the addition of TIP39, in *Pth2r*-/- mice, and in a previous study of chondrocytes (Panda et al., 2009) all strongly support the conclusion that PTH2R signaling can influence the production of decorin, collagen, MMPs, TIMPs and PGs. Addition of synthetic TIP39 peptide resulted in the phosphorylation of CREB, an effect previously

attributed to stimulation of the $G\alpha_s$–adenylyl cyclase–cAMP pathway, and a known factor in the control of decorin expression. We also showed that the expression of *MMP13* was strongly increased after wounding. MMP13 degrades collagen fibrils and contributes to remodeling wound tissue. However, the lack of TIP39 suppressed MMP13 production despite wounding. A previous report showed that PTH2R signaling directly downregulates the expression of SOX9 and increases MMPs (Panda et al., 2009); our TIP39 knockout data support this report.

Our data of decreased rate of closure of splinted wounds in TIP39-/- mice suggest the wound repair phenotype in part involves epithelial closure (**Figure 1f** and **S1d**), but this effect may also be due to an influence on the dermis. A direct effect on the epidermis is supported by our previously reported observations that PTH2R can influence calcium homeostasis and differentiation in keratinocytes, and that TIP39 increases intracellular calcium in keratinocytes (Sato et al., 2016). Keratinocyte migration is stimulated by increased intracellular calcium and the nuclear factor of activated T cells proteins, a family of Ca^{2+}-activated transcription factors (Brun et al., 2014; Fang et al., 1998; Jauliac et al., 2002; O'Connor et al., 2007). Thus, part of the wound repair phenotype we observed may be due to a direct effect of TIP39 on keratinocytes. However, GAGs and MMPs from the dermis may also indirectly influence keratinocyte migration. Thus, an indirect effect on epithelial closure due to an influence of

TIP39 signaling on the dermis is also possible. Taken together, our current and previously reported observations support the conclusion that TIP39–PTH2R signaling has an important influence on the function of both the epidermis and dermis. These effects of TIP39 and PTH2R point towards an important, multifaceted role in wound healing.

Our collagen gel cultures showed greatly increased decorin expression and supported prior observations of the importance of the 3D environment to model decorin expression in fibroblasts (Lee et al., 2004). This supported the phenotype observed in *Pth2r*-/- mice, in which PTH2R deficiency suppressed decorin expression in the dermis and subcutaneous tissue. Interestingly, our findings also suggest that GAGs may play a role in adipocyte differentiation. Adipocyte differentiation clearly decreased the expression of various PG genes compared with undifferentiated fibroblasts, and the main type of GAG produced was changed from HS to CS in the 3D collagen gels.

The role of the ECM, decorin and GAG in adipocyte differentiation is poorly understood. Hyaluronan, an unsulfated GAG, has been suggested to influence adipocyte differentiation (Ji et al., 2014). We observed that the expression of various PGs decreased with adipocyte differentiation in the 3D collagen gels compared with undifferentiated-fibroblasts. It is tempting to speculate that this reflects a shift in cell phenotype from a fibroblast dedicated to collagen matrix assembly to an adipocyte that does

not require a mechanically strong ECM, yet needs to accumulate lipid and also contribute to fighting infection (Zhang et al., 2015). Thus, activation of PTH2R could be predicted to drive an increase in dermal fibrosis and a decrease in adipogenesis.

In summary, this study demonstrates that TIP39-PTH2R signaling regulates decorin, a major component of the ECM, influences the structure of the dermis and the process of wound repair in mice. These observations open a new avenue of investigation that may be relevant to control of human dermal reorganization in processes such as development, aging and wound repair.

MATERIALS & METHODS

Recombinant peptides and antibodies

TIP39 peptides were obtained from Bachem Americas (Torrance, CA).Goat anti-Decorin (R&D, Minneapolis, MN), rabbit anti-CREB (Abcam, Cambridge, MA), rabbit anti-pCREB (Abcam), rabbit anti-LaminB1 (Abcam), goat anti-Perilipin (Abcam), goat anti-Actin (Santa Cruz, Dallas, TX) and rabbit anti-GAPDH(Abcam) were used as primary antibodies for immunoblotting or immunostaining. Alexa Fluor 488 or 594-conjugated donkey IgG (Thermo Fisher Scientific, Waltham, MA) were used as secondary antibodies for immunostaining.

Mice

6 - 18 weeks female C57BL/6, *Pth2r*-/-,*Tip39*-/- and their littermates were housed at the University Research Center at the University of California, San Diego. *Pth2r*-/- and *Tip39*-/- mice were obtained from Dr.Usdin (NIMH, Bethesda, MD). All animal experiments were approved by the UCSD Institutional Animal Care and Use Committee (IACUC).

Fibroblast-like precursor cells in Monolayer and 3D Collagen Culture

Primary human subcutaneous fibroblast-like precursor cells (preadipocytes) were obtained from Cell Applications (San Diego, CA) and primary mouse fibroblast/ preadipocyte cell line 3T3-L1 was purchased from ATCC (Manassas, VA) grown in preadipocyte growth medium

(Cell Applications) for up to seven passages under standard tissue culture conditions previously described(Zhang et al., 2015). Cells were cultured until 80 – 90% confluence and then replaced adipocyte differentiation medium (Cell Applications). Primary human keratinocytes and endothelial cells are cultured as previously described (Adase et al., 2016). For construction of 3T3-L1 containing-3D collagen plugs, type I collagen (Thermo Fisher Scientific) was solubilized in sterile-filtered Milli-Q water to a stock concentration of 5 mg/ml. The detail methods of 3T3-L1 collagen plug production is described in (Borkowski et al., 2013; Simpson et al., 2010). Gel formation occurred over 30 min at 37 °C, after which the gels were released from well sides with a pipette tip and from the bottom of the well with minimal shaking of the plate. After gel formation, 3mL of 10% FBS contained-DMEM (Thermo Fisher Scientific) was added on the 3D collagen plug. For inducing adipocyte differentiation, the outside medium was replaced from 10% FBS contained-DMEM to adipocyte differentiation medium at 48h after gel formation. 1μM TIP39 was mixed in both collagen plug and added to media.

Glycosaminoglycan and Proteoglycan Isolation by Anion Exchange Chromatography

3T3-L1 was seeded on 10cm dishes then cultured until 80 – 90% confluency. Adipocyte differentiation was induced for 3 days with or without 5 μM TIP39. The 30mL supernatant of each group was concentrated by Amicon Ultra 10K filter (Millipore, Billerica, MA). For digestion of the protein, the supernatant was incubated overnight with 0.1 mg/mL protease

(Sigma-Aldrich, St. Louis, MO) at 37 °C, followed by purification by anion exchange chromatography using DEAE sephacel (GE Healthcare, Chicago, IL). Columns were washed with a low-salt buffer (150 mM NaCl in 50 mM sodium acetate; pH 6.0) and eluted with 1 M NaCl. GAGs were desalted by PD10 (GE Healthcare). The detail method is described at the manual of GAG Release and Purification at UCSD Glycotechnology Core (http://glycotech.ucsd.edu/protocols/12_GAG%20Release%20and%20Analysis_Rev3.pdf) and (Muto et al., 2014). For isolation GAGs from 3D 3T3-L1 collagen gels, the plugs were solved in 3mL RIPA buffer for 10 min at 60 °C water bath. The solved-samples were vortexed by the highest speed and then centrifuged for 15 min at 15000 *g* 4 °C. Those supernatant were used for GAGs isolation.

Quantitative real-time PCR

Total RNA from mouse tissue samples and cultured keratinocytes was extracted, and cDNA was synthesized as previously described (Sato et al., 2016). TaqMan Gene Expression Assays (Thermo Fisher Scientific) were used to analyze expressions of mouse Decorin (gene symbol: *Dcn,* assay ID: Mm00514535_m1), mouse Adiponectin (gene symbol: *Adipoq,* assay ID: Mm00456425_m1), mouse Syndecan1 (gene symbol: *Sdc1,* assay ID: Mm00448918_m1), mouse Syndecan2 (gene symbol: *Sdc2,* assay ID: Mm04207492_m1),mouse Syndecan4 (gene symbol: *Sdc4,* assay ID: Mm00488527_m1), mouse Aggrecan (gene symbol: *Acan,*

assay ID: Mm00545794_m1), mouse Agrin (gene symbol: *Agrn,* assay ID: Mm01264855_m1), mouse Glypican1 (gene symbol: *Gpc1,* assay ID: Mm01264855_m1), mouse Glypican2 (gene symbol: *Gpc2,* assay ID: Mm00549650_m1), mouse Perlecan (gene symbol: *Hspg2,* assay ID: Mm01181173_g1), mouse Betaglycan (gene symbol: *Tgfbr3,* assay ID: Mm00803538_m1), as described by the manufacturer's instructions. Mouse β-actin (gene symbol: *Actb,* assay ID: Mm00607939_s1) was used as an internal control to validate RNA for each sample. Primer sequence of human PTH2 receptor, TIP39 and β-actin were below (*PTH2R* forward: 5'- CAGTTGGGCATGACACAAGG -3', *PTH2R* reverse: 5'-ACACAAAGAAACCCTGAAAGGA -3', *PTH2* forward: 5'-CCCCTTTCTGGTTCTCCACAG -3', *PTH2* reverse: 5'- GCATGTACGAGTTCAGCCA -3', *ACTB* forward: 5'- GCAAATGCTTCTAGGCGGAC -3', *ACTB* reverse: 5'-CGCATCTCATATTTGGAATGACT -3'). Each mRNA expression was calculated as the relative expression to β-actin mRNA, and all data are presented as fold change against each control (mean of non-stimulated cells).

Protein extraction and Immunoblotting

Samples were lysed in RIPA buffer as previously described (Sato et al., 2016). Protein concentrations were measured by BCA protein assay kit (Thermo Fischer Scientific). For immunoblotting, 10ug of protein was separated on a 10% Tris-Glycine precast gel (Bio-Rad,

Hercules, CA), transferred to PVDF membrane (Bio-Rad), followed by immunoblotting using indicated primary antibodies followed by fluorescent secondary antibodies (LICOR, Lincoln, NE) and imaging using fluorescent Odyssey System (LICOR). Densitometry was performed on scanned immunoblot images using the ImageJ software based on the measurement of the relative intensity. Values were further normalized to CREB levels in the respective blots.

Wound healing model

Two 6-mm full-thickness excisional wounds were created on the shaved dorsal surface of 8 week old female C57BL/6 wild-type, *TIP39*-/- and *TIP39*+/-mice under sterile conditions. Wound margins were then injected with or without TIP39 (250 ng/ 50 μL, 1.11 μM) every 24 h for 10 d after injury, and photographed every 48 h over that period, and wound area was manually traced by placing a transparent film over the wound and tracing the outline with a permanent marker. The method of wound measure has been described at (Ma et al., 2015). The tracing was then scanned and measured using an image analysis program (Image J Software 1.48v, NIH, Bethesda, MD). Three mice, each with 2 wounds (a total of 6 wounds) were studied in each treatment arm, and their rate of closure was analyzed. The study protocol included standard wound care as per IACUC guidelines. The splinted wound model was modified from (Galiano et al., 2004). A sterile 4-mm punch biopsy tool was used to create paired full-thickness wounds extending through the panniculus carnosus. A donut-shaped

splint with OD of 10mm and ID of 6mm was fashioned from a 0.5 mm-thick silicone sheet (Grace Bio-Laboratories, Bend, OR). The splint was placed so that the wound was fully visible in the center and interrupted 5-0 nylon sutures (Ethicon, Inc., Somerville, NJ) used to fix the splint to the skin. The animals were monitored throughout recovery from anesthesia and housed individually in the UCSD vivarium.

Immunofluorescence staining of cultured cells

Cells were fixed in -20°C cold methanol for 10 minutes then blocked with PBS containing 5% donkey serum at room temperature for 30 minutes. For sectioning of 3D collagen 3T3-L1, collagen plug was embedded in Optimal Cutting Temperature compound (Sakura Finetek USA, Torrance, CA) as previously described (Lee et al., 2004). Sectioning was performed at UC San Diego Moores Histology Core, La Jolla, CA. Detail immunostaining method was also described at (Sato et al., 2016). Anti-pCREB, anti-Perilipin, anti-Decorin and Alexa Fluor 488 or 594-conjugated donkey IgG (Thermo Fisher Scientific) were used at 1μg/mL. Cover slips were mounted using ProLong® Gold antifade Reagent with DAPI (Themo Fisher Scientific). Images were captured using a BX41 microscope (Olympus, Center Valley, PA).

Immunofluorescence for paraffin-embedded sections

The skin tissue samples were fixed in 10% formalin for 24 hours. Paraffin embedding and sectioning were performed at UC San Diego Moores Histology Core. 5-μm paraffin sections were deparaffinized and rehydrated before heat-induced antigen retrieval was performed in 10mM citrate buffer (pH 6.0) for 15 min at 121 degrees C (250 F). Immunostaining was performed as previously described (Sato et al., 2016). Anti-Decorin, anti-PTH2/TIP39 and Alexa Fluor 488 or 594-conjugated antibodies (donkey IgG) were used at 1μg/mL.

Van Gieson staining for paraffin-embedded sections

Van Gieson staining was performed at UC San Diego Moores Histology Core. Deparaffinized slides were stained using Elastic Stain Kit (Sigma-Aldrich) as its protocol (Procedure No. HT25). Elastic fibers and nuclear are stained blue to black, collagen is red and muscle/ other tissues are yellow.

RNA knockdown

Control and PTH2R Silencer® Select siRNA were purchased from Thermo Fisher Scientific. siRNA transfection was performed by manufacturer's instructions of Lipofectamine® RNAiMAX (MAN0007836, Thermo Fisher Scientific). Human fibroblast-like precursor cells were seeded on 24-well plates (fibroblast group: 2.0 x 10^4/ well, adipocyte group: 5.0 x 10^4/ well), and then incubated overnight. At day0, siRNA complex were transfected into cells with

or without adipocyte differentiation medium. Both siRNA and culture medium were replaced at day3. All samples were harvested at 5 days after transfection.

RNA-seq analysis

RNA sequence detail method is described at (Adase et al., 2016).RNA quality was checked using the R6K screen tape with an Agilent 2200 TapeStation (Agilent Technologies, Santa Clara, CA). RNA-seq libraries were prepared using the TruSeq Stranded mRNA (Illumina, San Diego, CA) and sequenced with the HiSeq2500, HighOutput v4 system (Illumina). All those processes were performed at the IGM Genomics Center, University of California, San Diego, La Jolla, CA. Gene analysis used Partek Gene Specific Analysis (GSA) run on the gene level with the following changes, Lowest maximum coverage: 1, Poisson: True, and TMM normalization. Gene filters used was false discovery rate (FDR) < 0.1. Heiarchal clustering and GO enrichment were performed using these filters utilizing Partek flow software.

Durometer measurements

Durometer measurements were made using a handheld dial durometer (HARDMATIC HH-300 Shore A; Mitsutoyo, Kanagawa, Japan). This durometer is provided with a peak retaining hand for error-free reading. Five consecutive durometer measurements were taken at each of five mice dorsal skin under anesthesia using isoflurane gas (2-5%, flow rate 1 L/min).

FIGURE LEGENDS

Figure 1. Activation of the PTH2 receptor enhances wound repair

(a) Wounds were made on C57BL/6 back skin by 6 mm punch, then injected with 50µl PBS or 250ng of TIP39 peptide dissolved in 50µl PBS. Peptide or PBS were injected to the wound margin daily. Wound closure rate (%) was calculated by Image J. Data are means ± SEM, n=6, **P<0.01 (Two way ANOVA with Bonferroni test). **(b - d)** Wounds were made on TIP39 knockout (TIP39-/-) or heterozygous (TIP39+/-) back skin by 6 mm punch. **(b)** Wound closure rate (%) was calculated as in (a). Data are means ± SEM, n=6, *P<0.05, **P<0.01 (Two way ANOVA with Bonferroni test) **(c)** Macro images of wound healing process. **(d)** Day 7 wounds were stained by van Gieson staining. Collagen bundles are stained red. * is granulation tissue **(e)** Macro images of splinted-wound healing process. Wounds were made on TIP39-/- or TIP39+/- back skin by 4mm punch. Yellow dotted line shows wound edge. **(f)** Epithelial closure rate of Day 3 splint-wounds were calculated in histological sections by Image J. [Re-epithelializarion (%) = Neo-epidermal diameter / Wound diameter × 100]. *P<0.05 (Student's *t*-test), n = 4.

Figure 2. PTH2 receptor signaling influences the extracellular matrix.

(a) Expression of TIP39 and PTH2R mRNA in various human primary cells. **(b)** PTH2R gene expression was analyzed by qPCR 5 days after silencing of PTH2R expression. (pAd: fibroblast-like precursor cells, Ad: adipocytes) **(c)** Silencing effects of PTH2R on fibroblasts or adipocytes were analyzed by RNA-seq gene profiling. Downregulated-genes with a significant FDR (FDR < 0.1) are represented. (n=4) **(d)** Top 10 GO terms of PTH2R silenced-fibroblasts and adipocytes. **(e)** Downregulated-genes in GO: 0030198 (extracellular matrix organization).**(f)** Heat map of gene expression in siPTH2R transfected- fibroblasts or adipocytes. qPCR data are means ± SEM of biological replicates from n=3. **P<0.001 (One way ANOVA with Dunnett's Multiple Comparison Test).

Figure 3. TIP39 increased decorin expression in fibroblasts contained-3D collagen gels.

(**a)** Day 0 normal skin and Day 10 wound samples from TIP39+/- or TIP39-/- were analyzed by qPCR. Data are means ± SEM, n=6, *P<0.05, ***P<0.001 (One way ANOVA with Dunnett's Multiple Comparison Test). **(b)** Gene expression of decorin in 3T3-L1 fibroblasts in 3D collagen gels supplied with or without 1 μM TIP39. **(c)** Immunoblotting of decorin in fibroblasts contained-3D collagen gels supplied with or without 1 μM TIP39. 3T3-L1 was

cultured in collagen gel for 7days. Data are means ± SEM, n=4. *P<0.05. **P<0.01 (Two way ANOVA with Bonferroni test).

Figure 4. TIP39 induced phosphorylation of CREB in fibroblasts

(a) Cytoplasmic and nuclear proteins were isolated from a monolayer of 3T3-L1 cells which were stimulated by 1.5 μM TIP39, and then analyzed by immunoblotting. **(b)** Relative abundance calculated by Image J of immunoblot of pCREB /CREB. Data are means ± SEM, n=3. **(c)** pCREB in 1μM TIP39 stimulated-fibroblasts. White bars, 20μm. **(d)** Immunofluorescence staining rate (%) of pCREB (green) /DAPI (blue). Data are means ± SEM, n=10. **P<0.001 (One way ANOVA with Dunnett's Multiple Comparison Test). **(e)** Immunofluorescence staining of decorin (red) with DAPI (blue).

Figure 5. Differentiating adipocytes produce chondroitin sulfate GAG.

(a,b) Monolayers of 3T3-L1 cells were differentiated for 3 days with or without 5 μM TIP39, and then supernatant collected from each group. The secreted-GAGs were extracted by DEAE column and 8% of the GAGs from total samples were used for monosaccharide

composition analysis using HPAEC-PAD. **(c)** GAGs were extracted from 3T3-L1 contained-collagen gels. A 25% of the total samples were used for gel electrophoresis. The right panel shows digested-GAGs by 20mU Heparinase 1 and 3 (3D pAd group) or 300mU chondroitinase ABC (3D Ad group) for 4h at 37 °C. The agarose gel was stained by stains-all. 3T3-L1 cells were cultured in collagen gels for 7 days with or without 1 μM TIP39. Adipocyte differentiation was started from 2 days after gel formation. (3D pAd: three-dimensional fibroblast-like precursor cells, 3D Ad: three-dimensional adipocytes) **(d)** mRNA expression of various core protein of GAGs in 3T3-L1 contained-collagen gel. Culture conditions were the same as (c). Data are means ± SEM, n=4. *P<0.05. **P<0.01 (One way ANOVA with Dunnett's Multiple Comparison Test).

Figure 6. The lack of PTH2 receptor signal decreased decorin production from dermal fibroblasts.

(a) Immunofluorescence staining of decorin (green) in the skin of *Pth2r*+/+ or *Pth2r*-/- mice. White bars, 20 μm. Blue is DAPI. **(b)** mRNA expression (qPCR) and **(c)** protein expression (immunoblotting) of decorin in *Pth2r*+/+ or *Pth2r*-/- dermis. Arrowheads show protein ladder (700 channel near-infrared detection). Decorin was detected in the 800 channel and Actin was

detected in the 700 channel. The right lane of dermis/subcutaneous sample was digested by 300mU chondroitinase ABC for 3h at 37 °C. Mouse dermis and subcutaneous tissues were separated from whole skin by 0.5M ammonium thiocyanate overnight at 4 °C. qPCR Data are means ± SEM, n=4 *P<0.05 (Student's *t*-test). **(d)** Reticular dermal collagen fibrils were observed by Transmission electron microscopy (TEM) in *Pth2r*+/+ or *Pth2r*-/- mice. White bars, 100 nm. Yellow arrows and * mark irregular collagen fibrils observed in *Pth2r*-/- mice. **(e)** Skin hardness of *Pth2r*-/- mice was measured by a Mitsutoyo durometer. **P<0.01 (Student's *t*-test).

CONFLICT OF INTEREST

Currently, RLG is a consultant and has equity interest in MatriSys and Sente Inc.

ACKNOWLEDGEMENTS

The authors would like to thank all the members of the Gallo laboratory for the input and stimulating conversations. We thank Y Jones at the UCSD EM Core for processing samples and helpful discussion of EM images. We thank UCSD Histology Core Facility for sectioning, H&E staining and van Gieson staining of paraffin samples.

AUTHOR CONTRIBUTIONS

E.S. designed and performed a majority of the experiments and wrote the manuscript. C.A.A. assisted with RNA-seq analysis, B.P.C. assisted with HPLC analysis, R.A.D. assisted with the splinted-wound model and L.Z. gave total experiment technical assistance, and reviewed the manuscript. R.L.G. supervised and designed experiments and wrote and prepared the manuscript. All authors reviewed and approved the final version of the manuscript.

FOOTNOTES

This work was supported in part by P01HL057345 and P01HL107150 to R.L.G and the UCSD Dermatologist Investigator Training Program 1T32AR062496 (JAS, CA). Raw and processed data discussed in this publication have been deposited in NCBI's Gene Expression Omnibus and are accessible through GEO Series accession number GSE89647 (https://www.ncbi.nlm.nih.gov/geo/query/acc.cgi?token=kpgpmoeqrhwzvyz&acc=GSE89647).

REFERENCES

Adase C.A., Borkowski A.W., Zhang L.J., Williams M.R., Sato E., Sanford J.A., et al. Non-coding Double-stranded RNA and Antimicrobial Peptide LL-37 Induce Growth Factor Expression from Keratinocytes and Endothelial Cells. *J Biol Chem*. 2016; 291: 11635-11646.

Akhurst R.J. A sweet link between TGFbeta and vascular disease? *Nat Genet*. 2006; 38: 400-401.

Atfi A.and Baron R. PTH battles TGF-beta in bone. *Nat Cell Biol*. 2010; 12: 205-207.

Birk D.E.and Silver F.H. Collagen fibrillogenesis in vitro: comparison of types I, II, and III. *Arch Biochem Biophys*. 1984; 235: 178-185.

Borkowski A.W., Park K., Uchida Y.and Gallo R.L. Activation of TLR3 in keratinocytes increases expression of genes involved in formation of the epidermis, lipid accumulation, and epidermal organelles. *J Invest Dermatol*. 2013; 133: 2031-2040.

Brett D. A Review of Collagen and Collagen-based Wound Dressings. *Wounds*. 2008; 20: 347-356.

Brun C., Demeaux A., Guaddachi F., Jean-Louis F., Oddos T., Bagot M., et al. T-plastin expression downstream to the calcineurin/NFAT pathway is involved in keratinocyte migration. *PLoS One*. 2014; 9: e104700.

Danielson K.G., Baribault H., Holmes D.F., Graham H., Kadler K.E.and Iozzo R.V. Targeted disruption of decorin leads to abnormal collagen fibril morphology and skin fragility. *J Cell Biol*. 1997; 136: 729-743.

Edwards I.J. Proteoglycans in prostate cancer. *Nat Rev Urol*. 2012; 9: 196-206.

Fang K.S., Farboud B., Nuccitelli R.and Isseroff R.R. Migration of human keratinocytes in electric fields requires growth factors and extracellular calcium. *J Invest Dermatol*. 1998; 111: 751-756.

Galiano R.D., Michaels J.t., Dobryansky M., Levine J.P.and Gurtner G.C. Quantitative and reproducible murine model of excisional wound healing. *Wound Repair Regen*. 2004; 12: 485-492.

Gallo R.L., Ono M., Povsic T., Page C., Eriksson E., Klagsbrun M., et al. Syndecans, cell surface heparan sulfate proteoglycans, are induced by a proline-rich antimicrobial peptide from wounds. *Proc Natl Acad Sci U S A*. 1994; 91: 11035-11039.

Jarvelainen H., Puolakkainen P., Pakkanen S., Brown E.L., Hook M., Iozzo R.V., et al. A role for decorin in cutaneous wound healing and angiogenesis. *Wound Repair Regen*. 2006; 14: 443-452.

Jauliac S., Lopez-Rodriguez C., Shaw L.M., Brown L.F., Rao A.and Toker A. The role of NFAT transcription factors in integrin-mediated carcinoma invasion. *Nat Cell Biol*. 2002; 4: 540-544.

Ji E., Jung M.Y., Park J.H., Kim S., Seo C.R., Park K.W., et al. Inhibition of adipogenesis in 3T3-L1 cells and suppression of abdominal fat accumulation in high-fat diet-feeding C57BL/6J mice after downregulation of hyaluronic acid. *Int J Obes (Lond)*. 2014; 38: 1035-1043.

Lee P.H., Trowbridge J.M., Taylor K.R., Morhenn V.B.and Gallo R.L. Dermatan sulfate proteoglycan and glycosaminoglycan synthesis is induced in fibroblasts by transfer to a three-dimensional extracellular environment. *J Biol Chem*. 2004; 279: 48640-48646.

Ma G.S., Aznar N., Kalogriopoulos N., Midde K.K., Lopez-Sanchez I., Sato E., et al. Therapeutic effects of cell-permeant peptides that activate G proteins downstream of growth factors. *Proc Natl Acad Sci U S A*. 2015; 112: E2602-2610.

Muto J., Morioka Y., Yamasaki K., Kim M., Garcia A., Carlin A.F., et al. Hyaluronan digestion controls DC migration from the skin. *J Clin Invest*. 2014; 124: 1309-1319.

Naylor E.C., Watson R.E.and Sherratt M.J. Molecular aspects of skin ageing. *Maturitas*. 2011; 69: 249-256.

O'Connor R.S., Mills S.T., Jones K.A., Ho S.N.and Pavlath G.K. A combinatorial role for NFAT5 in both myoblast migration and differentiation during skeletal muscle myogenesis. *J Cell Sci*. 2007; 120: 149-159.

Panda D., Goltzman D., Juppner H.and Karaplis A.C. TIP39/parathyroid hormone type 2 receptor signaling is a potent inhibitor of chondrocyte proliferation and differentiation. *Am J Physiol Endocrinol Metab*. 2009; 297: E1125-1136.

Qiu T., Wu X., Zhang F., Clemens T.L., Wan M.and Cao X. TGF-beta type II receptor phosphorylates PTH receptor to integrate bone remodelling signalling. *Nat Cell Biol*. 2010; 12: 224-234.

Ritter S.L.and Hall R.A. Fine-tuning of GPCR activity by receptor-interacting proteins. *Nat Rev Mol Cell Biol*. 2009; 10: 819-830.

Rostand K.S.and Esko J.D. Microbial adherence to and invasion through proteoglycans. *Infect Immun*. 1997; 65: 1-8.

Sarrazin S., Lamanna W.C.and Esko J.D. Heparan sulfate proteoglycans. *Cold Spring Harb Perspect Biol*. 2011; 3:

Sato E., Muto J., Zhang L.J., Adase C., Sanford J.A., Takahashi T., et al. The parathyroid hormone second receptor PTH2R, and its ligand tuberoinfundibular peptide of 39 residues TIP39, regulate intracellular calcium and influence keratinocyte differentiation. *J Invest Dermatol*. 2016:

Schaefer L.and Schaefer R.M. Proteoglycans: from structural compounds to signaling molecules. *Cell Tissue Res*. 2010; 339: 237-246.

Schmidt B.A.and Horsley V. Intradermal adipocytes mediate fibroblast recruitment during skin wound healing. *Development*. 2013; 140: 1517-1527.

Scott J.E.and Orford C.R. Dermatan sulphate-rich proteoglycan associates with rat tail-tendon collagen at the d band in the gap region. *Biochem J*. 1981; 197: 213-216.

Seo N.S., Hocking A.M., Hook M.and McQuillan D.J. Decorin core protein secretion is regulated by N-linked oligosaccharide and glycosaminoglycan additions. *J Biol Chem*. 2005; 280: 42774-42784.

Simpson C.L., Kojima S.and Getsios S. RNA interference in keratinocytes and an organotypic model of human epidermis. *Methods Mol Biol*. 2010; 585: 127-146.

Trowbridge J.M.and Gallo R.L. Dermatan sulfate: new functions from an old glycosaminoglycan. *Glycobiology*. 2002; 12: 117R-125R.

Usdin T.B., Hoare S.R., Wang T., Mezey E.and Kowalak J.A. TIP39: a new neuropeptide and PTH2-receptor agonist from hypothalamus. *Nat Neurosci*. 1999; 2: 941-943.

Wahab N.A., Parker S., Sraer J.D.and Mason R.M. The decorin high glucose response element and mechanism of its activation in human mesangial cells. *J Am Soc Nephrol*. 2000; 11: 1607-1619.

Weber I.T., Harrison R.W.and Iozzo R.V. Model structure of decorin and implications for collagen

fibrillogenesis. *J Biol Chem*. 1996; 271: 31767-31770.

Zhang L.J., Guerrero-Juarez C.F., Hata T., Bapat S.P., Ramos R., Plikus M.V., et al. Innate immunity. Dermal adipocytes protect against invasive Staphylococcus aureus skin infection. *Science*. 2015; 347: 67-71.

Figure 1.

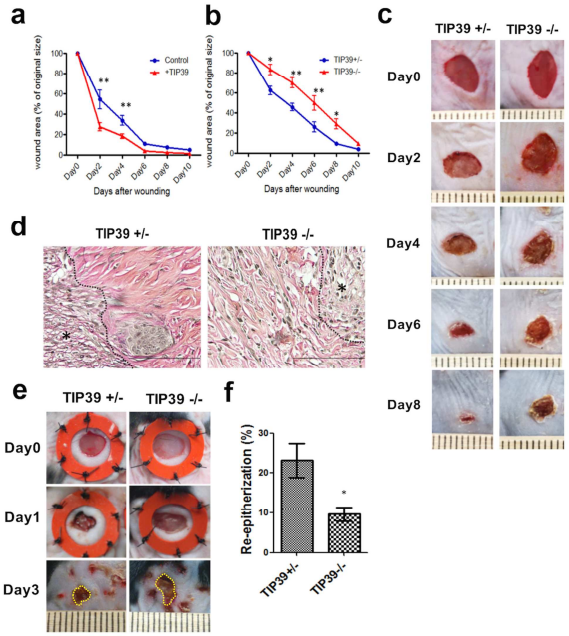

Figure 2.

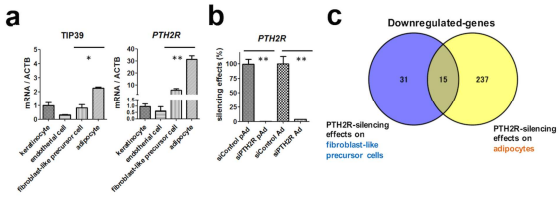

d

Fibroblast-like precursor cells

	Gene set	Description	P-value
1	GO:0044421	extracellular region part	1.81E-15
2	GO:0030198	extracellular matrix organization	3.32E-14
3	GO:0043062	extracellular structure organization	3.46E-14
4	GO:0022617	extracellular matrix disassembly	1.94E-13
5	GO:1901700	response to oxygen-containing compound	6.12E-13
6	GO:0010033	response to organic substance	6.13E-13
7	GO:0030574	collagen catabolic process	2.72E-12
8	GO:0042221	response to chemical	3.23E-12
9	GO:0005615	extracellular space	4.31E-12
10	GO:0044243	multicellular organismal catabolic process	6.22E-12

Adipocytes

	Gene set	Description	P-value
1	GO:0044421	extracellular region part	1.03E-37
2	GO:0044444	cytoplasmic part	9.73E-37
3	GO:0070062	extracellular exosome	9.45E-36
4	GO:0065010	extracellular membrane-bounded organelle	9.45E-36
5	GO:0043230	extracellular organelle	1.66E-35
6	GO:1903561	extracellular vesicle	1.66E-35
7	GO:0031988	membrane-bounded vesicle	4.18E-33
8	GO:0031982	vesicle	1.53E-31
9	GO:0044281	small molecule metabolic process	1.11E-29
10	GO:0044699	single-organism process	1.63E-28

e

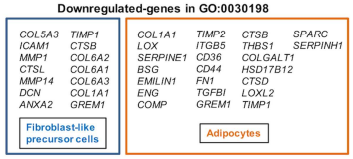

f

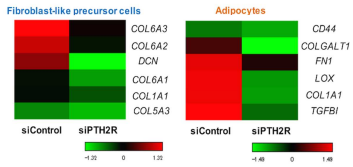

Figure 3.

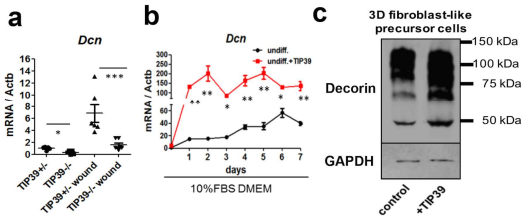

Figure 4.

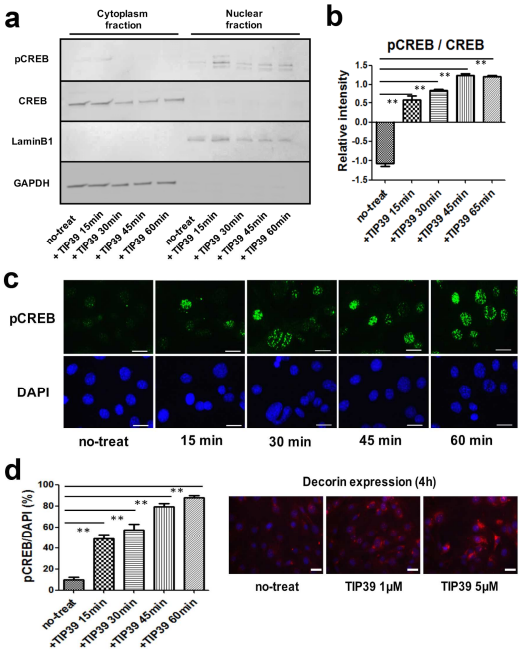

Figure 5.

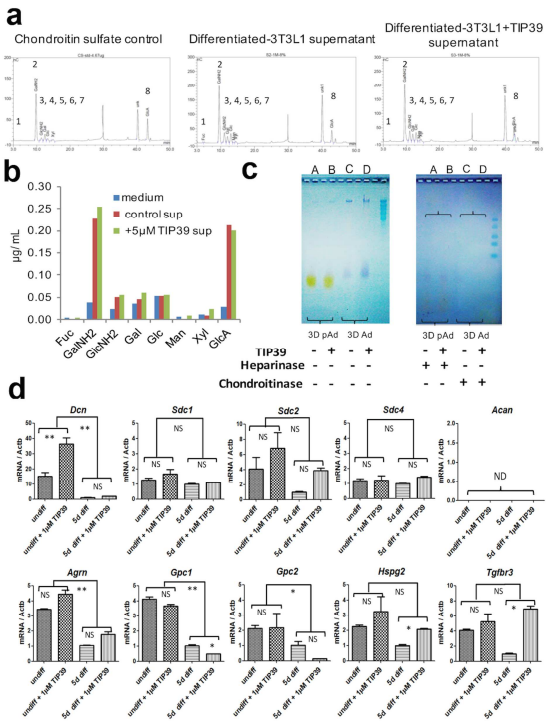

Figure 6.